



# Aging Impacts the Overall Connectivity Strength of Regions Critical for Information Transfer Among Brain Networks

Epifanio Bagarinao<sup>1</sup>, Hirohisa Watanabe<sup>1,2,3\*</sup>, Satoshi Maesawa<sup>1,4</sup>, Daisuke Mori<sup>1</sup>, Kazuhiro Hara<sup>3</sup>, Kazuya Kawabata<sup>3</sup>, Noritaka Yoneyama<sup>3</sup>, Reiko Ohdake<sup>3</sup>, Kazunori Imai<sup>3</sup>, Michihito Masuda<sup>3</sup>, Takamasa Yokoi<sup>3</sup>, Aya Ogura<sup>3</sup>, Toshiaki Taoka<sup>5</sup>, Shuji Koyama<sup>1</sup>, Hiroki C. Tanabe<sup>6</sup>, Masahisa Katsuno<sup>3</sup>, Toshihiko Wakabayashi<sup>4</sup>, Masafumi Kuzuya<sup>7,8</sup>, Minoru Hoshiyama<sup>1</sup>, Haruo Isoda<sup>1</sup>, Shinji Naganawa<sup>5</sup>, Norio Ozaki<sup>1,9</sup> and Gen Sobue<sup>1\*</sup>

<sup>1</sup> Brain and Mind Research Center, Nagoya University, Nagoya, Japan, <sup>2</sup> Department of Neurology, Fujita Health University School of Medicine, Toyoake, Japan, <sup>3</sup> Department of Neurology, Nagoya University Graduate School of Medicine, Nagoya, Japan, <sup>4</sup> Department of Neurosurgery, Nagoya University Graduate School of Medicine, Nagoya, Japan, <sup>5</sup> Department of Radiology, Nagoya University Graduate School of Medicine, Nagoya, Japan, <sup>6</sup> Department of Cognitive and Psychological Sciences, Graduate School of Informatics, Nagoya University, Nagoya, Japan, <sup>7</sup> Department of Community Healthcare and Geriatrics, Nagoya University Graduate School of Medicine, Nagoya, Japan, <sup>8</sup> Institutes of Innovation for Future Society, Nagoya University, Nagoya, Japan, <sup>9</sup> Department of Psychiatry, Nagoya University Graduate School of Medicine, Nagoya, Japan

## OPEN ACCESS

### Edited by:

Atsushi Takeda,  
Sendai Nishitaga National Hospital,  
Japan

### Reviewed by:

Agenor Limon,  
University of Texas Medical Branch  
at Galveston, United States  
Indira García Cordero,  
Universidad de San Andrés, Argentina

### \*Correspondence:

Gen Sobue  
sobueg@med.nagoya-u.ac.jp  
Hirohisa Watanabe  
nabe@med.nagoya-u.ac.jp

**Received:** 07 August 2020

**Accepted:** 09 October 2020

**Published:** 28 October 2020

### Citation:

Bagarinao E, Watanabe H, Maesawa S, Mori D, Hara K, Kawabata K, Yoneyama N, Ohdake R, Imai K, Masuda M, Yokoi T, Ogura A, Taoka T, Koyama S, Tanabe HC, Katsuno M, Wakabayashi T, Kuzuya M, Hoshiyama M, Isoda H, Naganawa S, Ozaki N and Sobue G (2020) Aging Impacts the Overall Connectivity Strength of Regions Critical for Information Transfer Among Brain Networks. *Front. Aging Neurosci.* 12:592469. doi: 10.3389/fnagi.2020.592469

Recent studies have demonstrated that connector hubs, regions considered critical for the flow of information across neural systems, are mostly involved in neurodegenerative dementia. Considering that aging can significantly affect the brain's intrinsic connectivity, identifying aging's impact on these regions' overall connection strength is important to differentiate changes associated with healthy aging from neurodegenerative disorders. Using resting state functional magnetic resonance imaging data from a carefully selected cohort of 175 healthy volunteers aging from 21 to 86 years old, we computed an intrinsic connectivity contrast (ICC) metric, which quantifies a region's overall connectivity strength, for whole brain, short-range, and long-range connections and examined age-related changes of this metric over the adult lifespan. We have identified a limited number of hub regions with ICC values that showed significant negative relationship with age. These include the medial precentral/midcingulate gyri and insula with both their short-range and long-range (and thus whole-brain) ICC values negatively associated with age, and the angular, middle frontal, and posterior cingulate gyri with their long-range ICC values mainly involved. Seed-based connectivity analyses further confirmed that these regions are connector hubs with connectivity profile that strongly overlapped with multiple large-scale brain networks. General cognitive performance was not associated with these hubs' ICC values. These findings suggest that even healthy aging could negatively impact the efficiency of regions critical for facilitating information transfer among different functional brain networks. The extent of the regions involved, however, was limited.

**Keywords:** aging, connector hubs, adult lifespan, intrinsic connectivity contrast, resting state fMRI

## INTRODUCTION

Studies have shown that the human brain is functionally organized into several large-scale networks, which can be identified using the spontaneous low frequency fluctuations of resting state functional magnetic resonance imaging (fMRI) data (Biswal et al., 1995; Greicius et al., 2003; Beckmann et al., 2005; Seeley et al., 2007). Some of these so-called resting state networks (RSNs), or their precursors, can already be identified even in the infant brain (Fransson et al., 2007; Smyser et al., 2010). These networks continue to mature with age and are continuously transformed across the life span (Tomasi and Volkow, 2012; Betzel et al., 2014; Sala-Llonch et al., 2015; Bagarinao et al., 2019). Characterizing the changes these RSNs undergo throughout normal development and aging is important as recent studies have indicated that RSN disruptions can also be associated with psychiatric (Greicius, 2008; Menon, 2011) and neurodegenerative disorders (Greicius et al., 2004; Hacker et al., 2012; Yao et al., 2014; Dai et al., 2015; Kawabata et al., 2018; Yokoi et al., 2018; Yoneyama et al., 2018; Ogura et al., 2019).

A number of brain regions called cortical hubs, characterized by numerous strong interconnections with several other regions, are considered critical for the flow of information within and between brain networks (Sporns et al., 2007). Prominent hub regions include the posterior cingulate, lateral temporal, lateral parietal, and medial/lateral prefrontal, many of which overlap with regions of the default mode network (Buckner et al., 2009). Given this critical role, hub regions are generally implicated in the anatomy of many disorders (Crossley et al., 2014). Its dysfunctions are also associated with behavioral and cognitive impairments in several neurological and psychiatric disorders (Buckner et al., 2009; van den Heuvel et al., 2013; van den Heuvel and Sporns, 2013; Dai et al., 2015) and could also provide novel insight into the pathomechanism of cognitive decline (Ogura et al., 2019).

Since the human brain processes information not only within adjacent areas but also from distant projections, recent studies have also investigated hub profiles in a distance-dependent manner (Sepulcre et al., 2010; Alexander-Bloch et al., 2013; Liang et al., 2013; Dai et al., 2015). Some hub regions were found to have high preference to local connectivity involving regions mostly in primary and secondary cortices (motor, somatosensory, auditory, visual, etc.), or long distance connectivity involving heteromodal regions in lateral parieto-temporal and frontal cortices, or both local and long distance connectivity involving regions which overlap with the default mode network (Sepulcre et al., 2010). By taking into account the distance of functional connections, certain vulnerabilities to distance-dependent connectivity changes can be identified. There are also differences in metabolic demands for long-range brain hubs, which require more energy, as compared to short-range hubs, making the former more vulnerable than the latter (Bullmore and Sporns, 2012).

Considering that aging can significantly affect the brain's intrinsic connectivity, characterizing age-related changes in the overall connectivity strength of hub regions is important in order to differentiate changes associated with healthy aging from that

due to neurodegenerative disorders. In this study, we examined aging's impact on the overall connection strength of hub regions. For this, we used resting state fMRI data to construct an intrinsic connectivity contrast (ICC) map (Martuzzi et al., 2011), which reflects each voxel's overall connectivity strength. Using a carefully selected cohort of healthy volunteers with age ranging from 21 to 86 years old, we first investigated the characteristics of the ICC map in a subgroup of young participants, and then examined how the ICC values change with age over the adult lifespan. In addition, we also examined whether some of the changes are distance-dependent (Euclidean) following earlier studies highlighting differences in the connectivity profile of hubs with respect to the distance of their connection. Finally, we performed seed-based connectivity analyses using as seed regions those with ICC values that showed significant association with age to identify the regions' connections to several well-known RSNs.

## MATERIALS AND METHODS

### Participants

Resting state fMRI data from 175 healthy volunteers (85 males/90 females) ranging in age from 21 to 86 years were included in the analysis. The included participants were carefully selected from those enrolled in our ongoing Brain and Mind Research Center Aging Cohort Study (Bagarinao et al., 2018, 2019) using the following exclusion criteria: 1) inability to complete the Japanese version of Addenbrooke's Cognitive Examination-Revised (ACE-R) assessment, 2) presence of structural abnormalities (e.g., asymptomatic cerebral infarction, benign brain tumor, white matter abnormalities, etc.) in structural MRI as identified by two Japanese board-certified neurologists (HW, KH) and a neurosurgeon (SM), 3) Mini-Mental State Examination (MMSE) score less than 26 or ACE-R total score less than 89, 4) head motion in resting state fMRI data with mean frame-wise displacement (FD) (Power et al., 2012) values greater than 0.2 mm, and 5) incomplete imaging data. Although MMSE score was also assessed, this score was only used for additional screening of the participants. The participants' characteristics are summarized in **Table 1**. All participants gave written informed consent before joining the study, which was approved by the Ethics Committee of Nagoya University Graduate School of Medicine and conformed to the Ethical Guidelines for Medical and Health Research Involving Human Subjects as endorsed by the Japanese Government.

### Magnetic Resonance Imaging (MRI) Data

All participants underwent MRI scanning at the Brain and Mind Research Center using a Siemens Magnetom Verio (Siemens, Erlangen, Germany) 3.0T scanner with a 32-channel head coil. For each participant, a high resolution T1-weighted (T1w) image and resting state fMRI data were acquired. The T1w image was acquired using a 3D MPRAGE (Magnetization Prepared Rapid Acquisition Gradient Echo, Siemens) pulse sequence (Mugler and Brookeman, 1990) with the following parameters: repetition time (TR)/MPRAGE repetition time = 7.4/2500 ms, echo time

TABLE 1 | Participants' characteristics.

Age Range	Count	M	F	Mean ACE-R (SD) score					
				Total	Attn	Mem	Flncy	Lang	Visu
20–29	39	25	14	96.5 (1.89)	17.9 (0.22)	24.2 (1.11)	13.8 (0.48)	24.9 (1.30)	15.7 (0.68)
30–39	21	10	11	97.9 (2.49)	18.0 (0.00)	25.0 (1.24)	13.4 (1.40)	25.4 (0.81)	16.0 (0.00)
40–49	19	11	8	96.4 (3.13)	17.9 (0.23)	24.3 (1.88)	13.4 (1.07)	25.0 (1.11)	15.7 (0.65)
50–59	34	12	22	97.4 (1.54)	17.9 (0.24)	24.6 (1.35)	13.7 (0.57)	25.4 (0.73)	15.8 (0.50)
60–69	35	14	21	96.1 (2.41)	17.9 (0.40)	23.7 (2.15)	13.8 (0.53)	25.2 (0.83)	15.5 (0.92)
70–79	26	13	13	94.8 (3.06)	17.8 (0.40)	23.6 (1.94)	13.1 (1.14)	24.8 (1.20)	15.5 (0.86)
80–89	1	0	1	91.0 (–)	17.0 (–)	20.0 (–)	14.0 (–)	25.0 (–)	15.0 (–)
Total	175	85	90						

SD, standard deviation; M, male; F, female; ACE-R, Addenbrooke's Cognitive Examination-Revised; Attn, attention; Mem, memory; Flncy, fluency; Lang, language; Visu, visuospatial.

(TE) = 2.48 ms, inversion time (TI) = 900 ms, flip angle (FA) = 8 degrees, field of view (FOV) = 256 mm, 256 × 256 matrix dimension, 192 sagittal slices with 1-mm thickness, in-plane voxel resolution of 1.0 × 1.0 mm<sup>2</sup>, and total scan time of 5 min and 49 s. For the resting state fMRI data, an ascending gradient echo (GE) echo planar imaging (EPI) pulse sequence was used with the following imaging parameters: TR = 2.5 s, TE = 30 ms, FOV = 192 mm, 64 × 64 matrix dimension, FA = 80 degrees, 39 transverse slices with a 0.5-mm inter-slice interval and 3-mm slice thickness, and total scan time of 8 min and 15 s. During resting state fMRI scan, participants were instructed to close their eyes but not to fall asleep.

## Image Preprocessing

All images were preprocessed using Statistical Parametric Mapping (SPM12, Wellcome Trust Center for Neuroimaging, London, United Kingdom) running on Matlab (R2016b, MathWorks, Natick, MA, United States). Using SPM12's segmentation approach (Ashburner and Friston, 2005), the T1w images were segmented into component images including gray matter (GM), white matter (WM), cerebrospinal fluid (CSF), and other non-brain tissue components. Bias-corrected T1w images and the transformation information from subject space to the Montreal Neuroimaging Institute (MNI) space were also obtained. For each resting state fMRI data, the first five volumes in the series were removed. Based on our previous work, this number is already sufficient to account for the initial BOLD signal instability. The remaining images were then slice-time corrected relative to the middle slice (slice 20), and then realigned to the mean image, computed after initially realigning the images relative to the first image. The mean image, together with the realigned images, were then co-registered to the bias-corrected T1w image, normalized to the MNI space using the transformation information obtained during segmentation, resampled to an isotropic 2 × 2 × 2 mm<sup>3</sup> voxel resolution, and smoothed using an isotropic 8-mm full-width-at-half-maximum 3-dimensional Gaussian filter. The preprocessed images were then corrected for head motion and contribution from other nuisance signals. In particular, we regressed out 24 motion-related signals given by  $[R_t, R_t^2, R_t - 1, \text{ and } R_t - 1^2]$ , where

$R_t = [x_t, y_t, z_t, \alpha_t, \beta_t, \gamma_t]$  represents the estimated motion parameters ( $x, y, \text{ and } z$  for translations and  $\alpha, \beta, \text{ and } \gamma$  for rotations about  $x, y, \text{ and } z$ , respectively) at time  $t$ . Mean signals from spherical regions of interest (radius = 4 mm) within the CSF and WM, the global signal, as well as derivatives of these signals were also removed. Finally, a bandpass filter within the frequency range from 0.01 to 0.1 Hz was also applied. These additional image preprocessing steps were performed using functions available in Matlab.

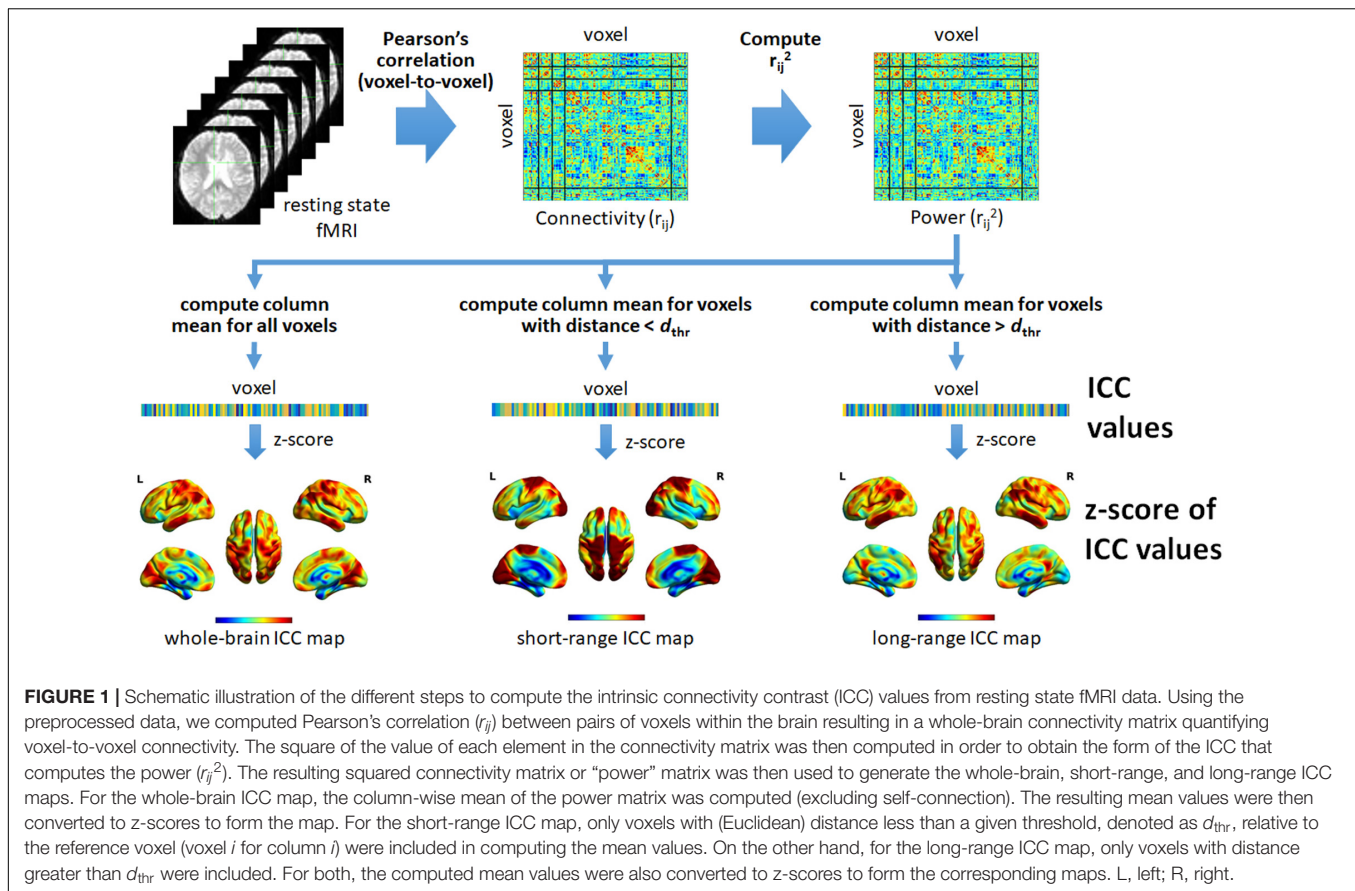
## Intrinsic Connectivity Contrast

From the preprocessed functional images, we computed the voxel-wise ICC (Martuzzi et al., 2011) using Matlab. Specifically, we used the form of the ICC that computes the power (ICC-p<sub>th</sub>) with the threshold set to 0 and computed using the following formula:

$$ICC(i) = \frac{1}{n} \sum_{j \neq i}^n r(i, j)^2$$

where  $r(i, j)$  is the connectivity value between voxels  $i$  and  $j$  and  $n$  is the number of voxels. To exclude unnecessary voxels, we limit our analysis to only include GM-relevant voxels. For this, we generated a GM mask by applying a threshold value of 0.2 to SPM12's GM tissue probability map. Voxels with values exceeding this threshold were included in the GM mask. The ICC values of all voxels within the mask were then computed resulting in a map of ICC values. Finally, the ICC values were standardized by subtracting the mean ICC computed from all voxels in the image, and dividing the difference by the standard deviation. This conversion to  $z$ -score does not affect the topography of the individual maps but enables the maps to be averaged and compared across participants (Buckner et al., 2009).

Distance-dependent ICC values were also computed. For the short-range ICC values, only voxels within distance  $d_{thr}$  (Euclidean) from the reference voxel were included in the computation. On the other hand, for long-range ICC values, only voxels with distance greater than  $d_{thr}$  were included. In this study, we used  $d_{thr} = 75$  mm to be consistent with the value used in previous studies (Achard et al., 2006; He et al., 2007). The different steps in computing the different ICC maps are summarized in **Figure 1**.



## Statistical Analyses

Although hub regions identified using the network metric called degree are known (Buckner et al., 2009), hub regions identified using ICC are yet to be characterized. Given this, we first profiled the spatial distribution of ICC values across the brain for whole-brain, short-range, and long-range connections. For this analysis, we used data from a subset of participants with age less than 40 years old ( $N = 60$ ). We performed one-sample  $t$ -tests of the ICC maps for the whole brain, long-range, and short-range ICC values using SPM12. To identify voxels with the most significant ICC values, we applied a more stringent  $p$ -value threshold equal to 0.05 corrected for multiple comparisons using a family-wise error (FWE) rate and cluster size equal to or greater than 25 voxels to the resulting statistical maps. We note that this analysis is primarily aimed to establish the spatial profile of the ICC metric across the whole brain, rather than to make comparisons across different age groups. To examine age-related changes in ICC values, which is our primary goal, we used regression analysis as described next.

We examined the relationship between ICC values and age and cognitive performance using data from all participants. Since all participants were cognitively normal, the variability of several ACE-R sub-scores were very limited (Table 1), preventing us to investigate associations at specific cognitive subdomains. We therefore used the ACE-R total score as

the metric representing general cognitive performance. We used a linear regression model with age and ACE-R total score as regressors. We also included sex and the mean FD values estimated from the realignment parameters (Power et al., 2012) as regressors of no interest to account for potential sex differences and the residual effects of head motion. Regression coefficients were estimated using SPM12. Generated statistical maps were thresholded using a  $p$ -value equal to 0.05 corrected for multiple comparisons using FWE at the cluster level (FWE<sub>c</sub>) with a cluster defining threshold (CDT) set at  $p = 0.001$ .

## Seed-Based Connectivity Analysis and RSN Overlap Ratio

We also performed additional seed-based connectivity analyses using regions with ICC values that showed significant relationship with age to quantify the regions' connectivity relative to well-known RSNs. This would be useful in identifying connector hubs from non-connector hubs as the former will be significantly connected to not just one but multiple RSNs. Spherical seed regions-of-interest (ROIs) with centers located at the MNI coordinates of the significant clusters' peak locations and radius equal to 4 mm were used. For each seed ROI, its mean time series was extracted and correlated to that of all voxels within the brain (whole-brain connections) to generate its corresponding functional

connectivity map. Using the generated connectivity maps from participants in the young adult subgroup, a one-sample *t*-test was then performed. The resulting statistical map was corrected for multiple comparisons using FWE<sub>c</sub>  $p < 0.05$  with a CDT set at  $p = 0.001$  to obtain the group-level functional connectivity map of the given ROI. To quantify the seed ROI's connectivity with several RSNs, we estimated the spatial overlap of the thresholded statistical map with well-known RSNs. For this, we used the 14 RSN templates from Shirer et al. (2012) as reference and computed an RSN overlap ratio  $R$  (Bagarinao et al., 2020) using the following equation:

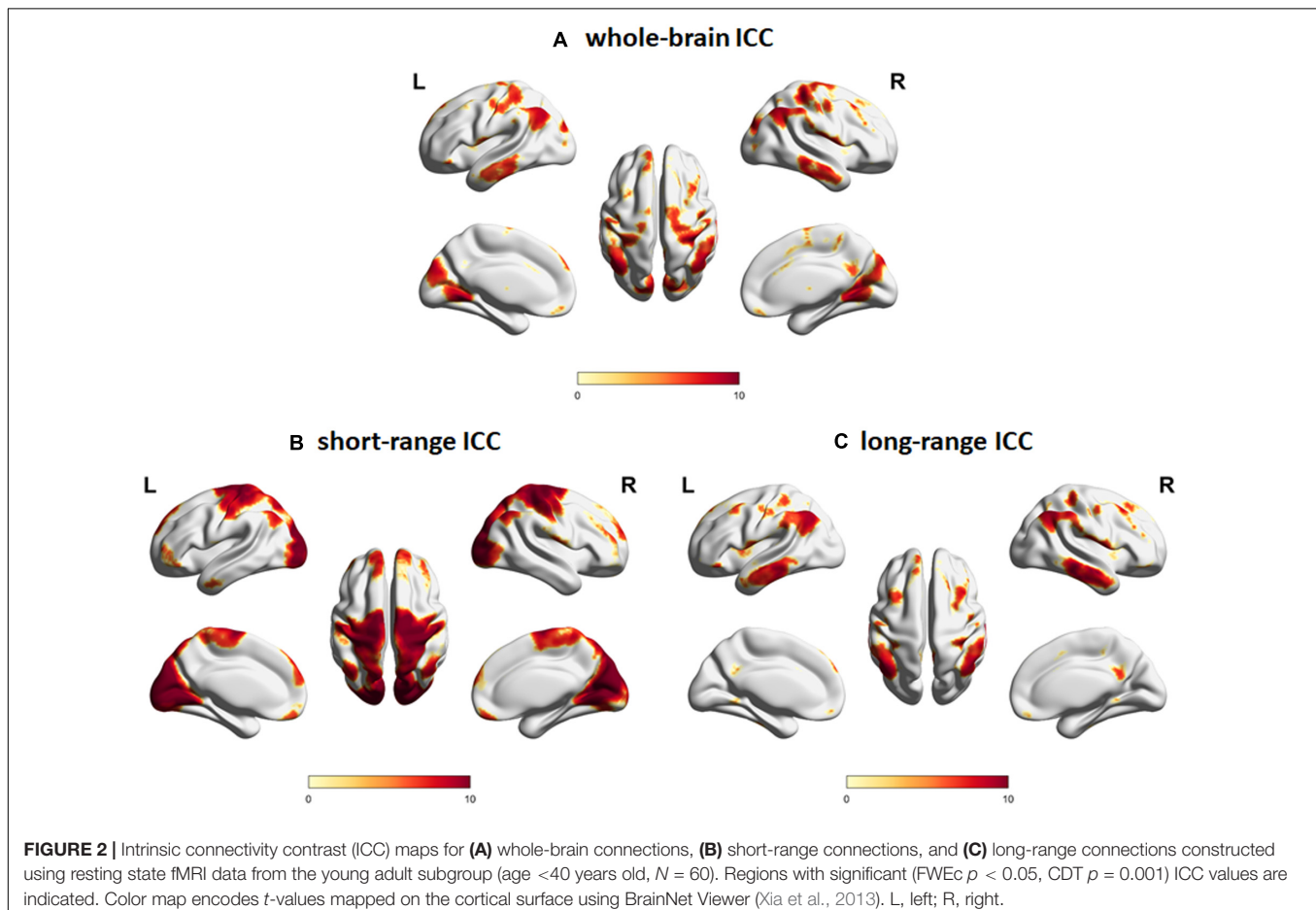
$$R = \frac{N_{\text{overlap}}}{N_{\text{RSN}}},$$

where  $N_{\text{overlap}}$  is the number of voxels in the RSN template that overlapped with the FWE<sub>c</sub>-corrected statistical map of the ROI, and  $N_{\text{RSN}}$  is the total number of voxels in the RSN template. An overlap ratio of 1 means that the RSN template is fully within the corrected connectivity map of the given seed ROI ( $N_{\text{overlap}} = N_{\text{RSN}}$ ), whereas a value of 0 means no overlap at all ( $N_{\text{overlap}} = 0$ ). We used the RSN overlap ratio to identify the different RSNs where the seed ROI has significant functional connection.

## RESULTS

### ICC Characteristics in Young Adult Participants

We first characterized the spatial distribution of the ICC maps in a subgroup of young adult participants. Whole-brain ICC maps identified hub regions showing significant ICC values in the bilateral middle frontal gyrus, angular gyrus, middle temporal gyrus, precuneus, medial superior frontal gyrus, lateral orbital gyrus, lingual gyrus, and central operculum, among others (**Figure 2A**). For the distance-dependent ICC maps, cortical hubs characterized by significant short-range ICC values were observed in regions associated with primary processing networks (visual and sensorimotor) as well as in bilateral medial superior frontal gyrus, lateral orbital gyrus/orbital part of the inferior frontal gyrus, lateral parietal, right central operculum, and cerebellum (**Figure 2B**). In contrast, cortical hubs characterized by significant long-range ICC values were observed in regions associated with the core neurocognitive networks (default mode, salience, and executive control) such as the bilateral middle frontal gyrus, angular/supramarginal gyrus, inferior/middle temporal gyrus, precuneus/posterior cingulate gyrus, and midcingulate gyrus, among others (**Figure 2C**). MNI coordinates of the peak locations and sizes of the significant



clusters are given in **Supplementary Tables S1–S3** for whole-brain, short-range, and long-range ICC values, respectively.

### Relationship Between ICC Values and Age

Regions with whole-brain ICC values that showed significant negative linear relationship with age included the bilateral insula, bilateral medial segment of the precentral gyrus/midcingulate, left middle temporal gyrus, left anterior cingulate gyrus, and right angular gyrus (**Figure 3a**). Age-related changes in whole-brain ICC values in the bilateral insula and the medial segment of

the precentral gyrus/midcingulate gyrus were influenced by both the short-range and long-range ICC values, which also showed significant negative relationship with age (**Figures 4a, 5a**). On the other hand, age-related changes in whole-brain ICC values in the left anterior cingulate gyrus and middle temporal gyrus were mostly influenced by the short-range ICC values (**Figure 4a**), whereas that in the right angular gyrus by the long-range ICC values (**Figure 5a**). A region in the left fusiform gyrus has only short-range ICC values that showed significant negative relationship with age (**Figure 4a**). In contrast, regions in the right central operculum, bilateral angular gyrus, left middle frontal

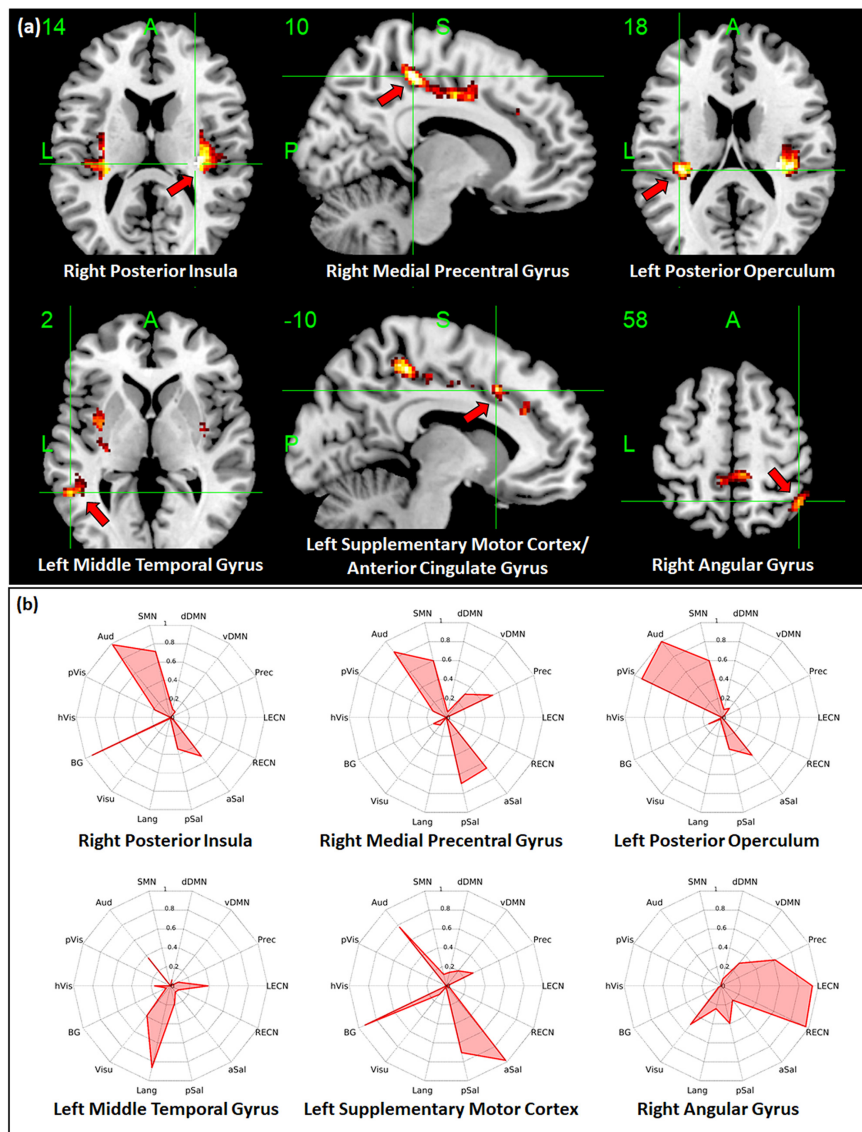


**FIGURE 3 |** Relationship between whole-brain intrinsic connectivity contrast (ICC) values and age. **(a)** Regions with whole-brain ICC values that showed significant (FWEc  $p < 0.05$ , CDT  $p = 0.001$ ) negative linear relationship with age. **(b)** Spider plots of the overlap ratio quantifying the connection between the 14 canonical resting state networks and the regions shown in **(a)**. dDMN, dorsal default mode network; vDMN, ventral default mode network; Prec, precuneus network; LECN, left executive control network; RECN, right executive control network; aSal, anterior salience network; pSal, posterior salience network; Lang, language network; Visu, visuospatial (dorsal attention) network; BG, basal ganglia network; hVis, high visual network; pVis, primary visual network; Aud, auditory network; SMN, sensorimotor network; R, right; L, left.

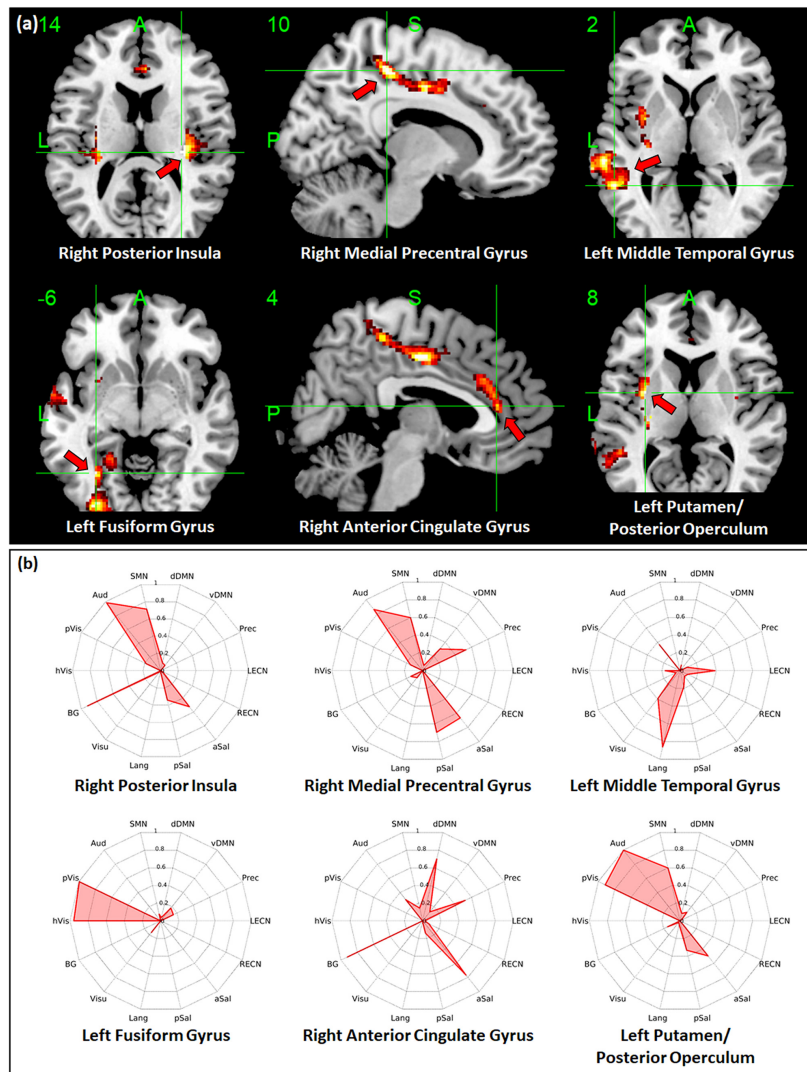


**FIGURE 4 |** Relationship between short-range intrinsic connectivity contrast (ICC) values and age. **(a)** Regions with short-range ICC values that showed significant (FWE $p < 0.05$ , CDT  $p = 0.001$ ) negative linear relationship with age. **(b)** Spider plots of the overlap ratio quantifying the connection between the 14 canonical resting state networks and the regions shown in **(a)**. dDMN, dorsal default mode network; vDMN, ventral default mode network; Prec, precuneus network; LECN, left executive control network; RECN, right executive control network; aSal, anterior salience network; pSal, posterior salience network; Lang, language network; Visu, visuospatial (dorsal attention) network; BG, basal ganglia network; hVis, high visual network; pVis, primary visual network; Aud, auditory network; SMN, sensorimotor network; R, right; L, left.

gyrus, and posterior cingulate gyrus have only long-range ICC values that showed significant negative linear relationship with age (Figure 5a).

Regions in the bilateral caudate and right cerebellum have whole-brain, short-range, and long-range ICC values that showed significant positive relationship with age. Other regions with ICC values exhibiting positive association with age included the right thalamus and left hippocampus for whole-brain ICC values, the right lingual gyrus for both whole-brain and long-range ICC values, and the right planum polare/temporal pole for both whole-brain and short-range ICC values. Peak locations in MNI coordinates and sizes of the significant clusters are given in

Tables 2–4 for whole-brain, short-range, and long-range ICC values, respectively.

### Overlap of Seed-Based Connectivity Maps With Large-Scale RSNs

To quantify the connectivity between regions with ICC values showing significant negative relationship with age and large-scale functional networks, we computed the overlap ratio between the estimated connectivity map of each region and 14 well-known RSN templates. Spider plots of the overlap ratio for the different seed ROIs showing age-related changes in whole-brain, short-range, and long-range ICC values are shown in Figures 3b, 4b, and 5b, respectively. From these

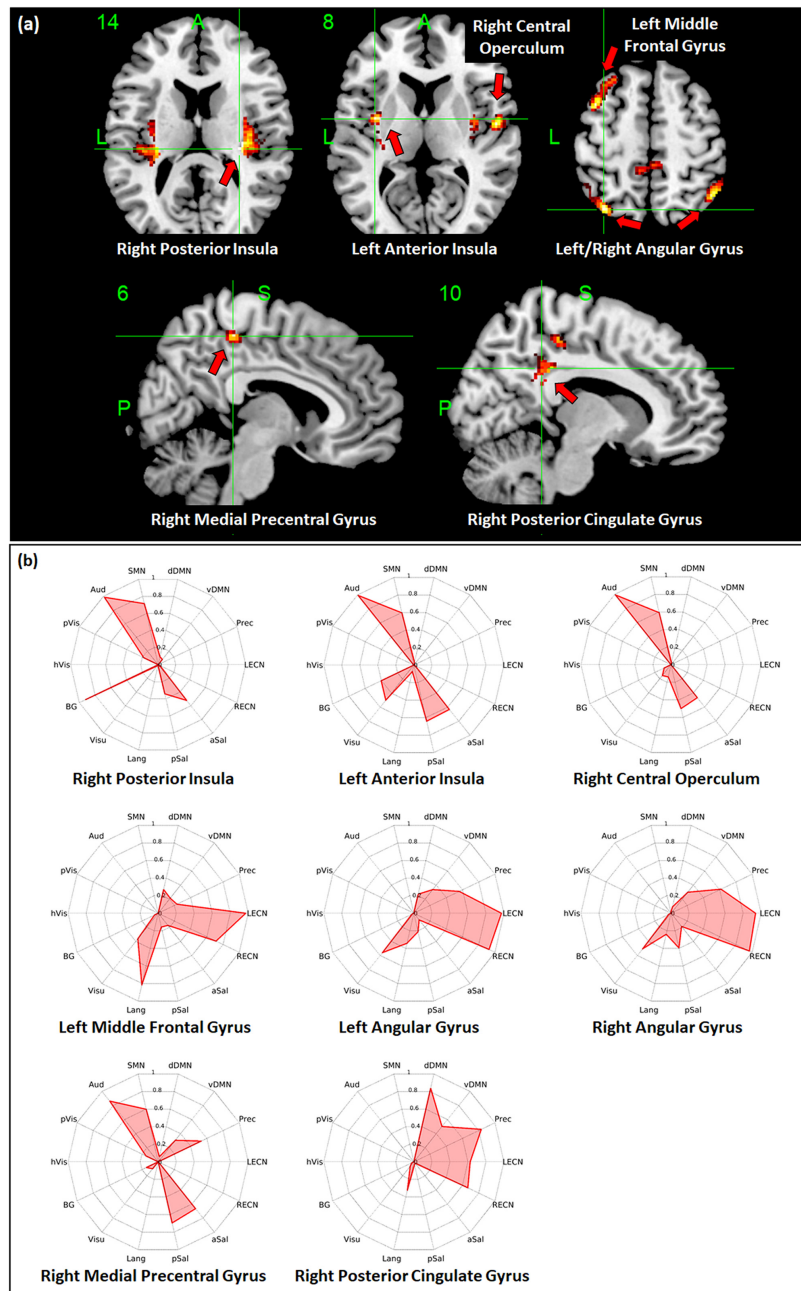


**FIGURE 5 |** Relationship between long-range intrinsic connectivity contrast (ICC) values and age. **(a)** Regions with long-range ICC values that showed significant (FWEc  $p < 0.05$ , CDT  $p = 0.001$ ) negative linear relationship with age. **(b)** Spider plots of the overlap ratio quantifying the connection between the 14 canonical resting state networks and the regions shown in **(a)**. dDMN, dorsal default mode network; vDMN, ventral default mode network; Prec, precuneus network; LECN, left executive control network; RECN, right executive control network; aSal, anterior salience network; pSal, posterior salience network; Lang, language network; Visu, visuospatial (dorsal attention) network; BG, basal ganglia network; hVis, high visual network; pVis, primary visual network; Aud, auditory network; SMN, sensorimotor network; R, right; L, left.

figures, it is evident that the identified ROIs have connectivity profiles that overlapped with not just one but several RSNs indicating that these regions are mostly connector hub regions. Regions with whole-brain, short-range, and long-range ICC values that showed significant negative relationship with age (right posterior insula, right medial precentral gyrus, and

left posterior operculum) had strong overlap with primary processing networks (sensorimotor, auditory, and visual) and salience network (**Figure 3b**). In contrast, regions with long-range ICC values that showed significant negative relationship with age (bilateral angular gyrus, left middle frontal gyrus, and right posterior cingulate gyrus) were strongly connected

**TABLE 2** | Regions showing significant (FWE $p < 0.05$ , CDT  $p = 0.001$ ) relationship between whole-brain ICC values and age and ACE-R total score.

Contrast	X	Y	Z	z-Value	Cluster size	Area	Other within cluster peaks
Age (+)	-10	14	2	6.61	436	L Cau	
	14	16	6	6.17	267	R Cau	
	14	-34	20	6.1	149	R ThP	
	34	-34	-40	5.47	371	R Cer	
	4	-98	-4	4.86	182	R LiG	R OCP, L OCP
	44	-10	-10	4.77	179	R PP	R TMP
	-18	-44	16	4.63	249	L Hip	
Age (-)	34	18	-42	4.48	168	R TMP	
	30	-24	14	5.99	349	R Plns	R Alns
	10	-32	52	5.48	955	R MPrG	R MCgG, L MPrG
	-36	-28	18	5.02	446	L PO	L Alns, L Plns
	-10	16	40	4.62	180	L SMC	L ACgG, R ACgG
	-54	-48	2	4.4	136	L MTG	L STG
	44	-54	58	4.34	128	R AnG	R SPL
ACE-R (+)	-34	-74	-16	4.47	380	L OFuG	L Calc
	18	-76	6	4.35	744	R Calc	R OFuG, R LiG
	-18	-86	26	4.29	425	L SOG	L OCP
	-30	-24	62	4.08	220	L PrG	L PoG
	-20	-54	0	3.9	121	L LiG	
	-10	-72	-56	4.21	218	L Cer	

Cau, caudate; ThP, thalamus proper; Cer, cerebellum; LiG, lingual gyrus; OCP, occipital pole; PP, planum polare; TMP, temporal pole; Hip, hippocampus; Plns, posterior insula; Alns, anterior insula; MPrG, medial precentral gyrus; MCgG, midcingulate gyrus; PO, posterior operculum; SMC, supplementary motor cortex; ACgG, anterior cingulate gyrus; MTG, middle temporal gyrus; STG, superior temporal gyrus; AnG, angular gyrus; SPL, superior parietal lobule; OFuG, occipital fusiform gyrus; Calc, calcarine; SOG, superior occipital gyrus; PrG, precentral gyrus; PoG, postcentral gyrus; ACE-R, Addenbrooke's Cognitive Examination-Revised; L, left; R, right.

with control (visuospatial, executive control, and salience) and default mode networks.

## Relationship Between ICC Values and ACE-R Total Score

From Tables 2–4, one can see that some regions in the visual cortex (occipital fusiform gyrus, calcarine, and superior occipital gyrus), sensorimotor cortex (left precentral and postcentral gyri), and cerebellum have whole-brain, short-range, and long-range ICC values that positively correlated with ACE-R total score. All of the regions do not overlap with those showing significant negative relationship with age except the one in the left lingual gyrus with short-range ICC values that showed significant positive relationship with ACE-R total score and negative relationship with age.

## DISCUSSION

Using resting state fMRI, we estimated ICC values at the voxel-level. We first characterized whole-brain as well as distance-dependent ICC maps in a subgroup of young adult participants, and then examined how the ICC values change with age over the adult lifespan. Our results showed that regions with significantly higher ICC values were generally consistent with previously

identified hubs (Buckner et al., 2009; Sepulcre et al., 2010), thus validating the use of the ICC metric as an effective measure to characterize hub regions. Furthermore, we have identified a limited number of regions with ICC values that showed significant negative relationship with age. These include regions in the medial precentral gyrus and insula with whole-brain as well as distance-dependent ICC values that showed significant negative relationship with age. Seed-based connectivity analyses have indicated that these regions have connectivity maps that strongly overlapped with both primary processing and salience networks. Regions in the angular gyrus, middle frontal gyrus, and posterior cingulate gyrus have also ICC values, primarily with their long-range connections, that exhibited significant negative relationship with age. These regions' connectivity maps strongly overlapped with control (visuospatial, salience, and executive control) and default mode networks. Taken together, these findings suggest that even healthy aging could negatively impact the overall connectivity strength of connector hubs, regions critical for the exchange of information across different brain networks. The extent, however, was limited.

Several studies have investigated the effect of normal aging in the connectivity of large-scale brain networks and the organization of functional brain networks across the lifespan (Andrews-Hanna et al., 2007; Jones et al., 2011; Tomasi and Volkow, 2012; Betzel et al., 2014; Bagarinao et al., 2019). Age-related connectivity changes were found to be widespread across many networks. Commonly observed changes included decreases in connectivity within large-scale functional networks, whereas connectivity between networks tended to increase (Betzel et al., 2014; Bagarinao et al., 2019). Using graph-theoretic framework, other studies have also indicated greater functional network reorganization in the brain with increasing age reflected in age-related alterations in network metrics such as modularity, local efficiency and global efficiency (Achard and Bullmore, 2007; Chan et al., 2014; Song et al., 2014; Geerligts et al., 2015). Our own study (Bagarinao et al., 2019) has also shown that the aging brain is characterized by decreasing path length, increasing global efficiency and network degree, and decreasing betweenness, indicating a tendency of the aging brain to re-organize toward a more integrated functional network with, probably, a more random topology (Bullmore and Sporns, 2012). Overall, widespread connectivity alterations and functional network reorganization have been consistently observed with aging.

In this study, we focused on aging's effect on a specialized set of regions called hubs, which still remains largely unexplored. For this, we used ICC, a voxel-level metric, which enabled us to account for both the presence of connections among voxels as well as the strength of these connections (Martuzzi et al., 2011). Since ICC can be computed at the voxel level, this approach also avoided parcelation-related biases on the estimation of metrics characterizing brain networks (Smith et al., 2011). With ICC, we have also avoided the problem of identifying the appropriate connectivity threshold to use in order to define the network since ICC can be estimated without applying any threshold. Moreover, since aging could affect connectivity strength in a continuous manner, estimating the overall connectivity strength as quantified by the ICC values, rather than just the number of connections,

**TABLE 3** | Regions showing significant (FWEc  $p < 0.05$ , CDT  $p = 0.001$ ) relationship between short-range ICC values and age and ACE-R total score.

Contrast	X	Y	Z	z-Value	Cluster size	Area	Other within cluster peaks
Age (+)	-10	14	2	6.49	467	L Cau	
	14	16	6	6.15	382	R Cau	
	-46	-8	-8	5.42	171	L PP	
	36	-34	-38	5.24	371	R Cer	R FuG
	46	-6	-10	4.97	378	R PP	R TMP
Age (-)	34	18	-44	4.95	204	R TMP	
	30	-24	14	5.77	219	R Plns	R Pu
	10	-32	52	5.41	1046	R MPrG	R MCgG, L MCgG
	-32	-58	-6	4.96	625	L FuG	L IOG, L OFuG
	-54	-48	2	4.93	675	L MTG	L STG
ACE-R (+)	-32	0	8	4.8	384	L Pu	L PO, L Plns
	4	36	14	4.26	408	R ACgG	L ACgG, L SMC
	-20	-86	28	4.45	1,426	L SOG	R Calc
	-18	-86	-16	4	226	L OFuG	
	-20	-54	0	3.86	217	L LiG	L Calc
ACE-R (-)	22	2	60	4.76	174	R SFG	

Cau, caudate; PP, planum polare; Cer, cerebellum; FuG, fusiform gyrus; TMP, temporal pole; Plns, posterior insula; Pu, putamen; MPrG, medial precentral gyrus; MCgG, midcingulate gyrus; IOG, inferior occipital gyrus; OFuG, occipital fusiform gyrus; MTG, middle temporal gyrus; STG, superior temporal gyrus; PO, posterior operculum; ACgG, anterior cingulate gyrus; SMC, supplementary motor cortex; SOG, superior occipital gyrus; Calc, calcarine; LiG, lingual gyrus; SFG, superior frontal gyrus; ACE-R, Addenbrooke's Cognitive Examination-Revised; L, left; R, right.

**TABLE 4** | Regions showing significant (FWEc  $p < 0.05$ , CDT  $p = 0.001$ ) relationship between long-range ICC values and age and ACE-R total score.

Contrast	X	Y	Z	z-Value	Cluster size	Area	Other within cluster peaks
Age (+)	-10	14	2	6.31	476	L Cau	
	14	16	6	5.99	230	R Cau	
	34	-34	-40	5.03	165	R Cer	R FuG
	4	-98	-4	4.78	309	R LiG	R OCP, L LiG
Age (-)	30	-24	14	5.51	339	R Plns	R Alns, R PO
	52	-6	6	5.04	146	R CO	
	-36	-2	8	4.77	330	L Alns	L PO, L Plns
	-34	-68	56	4.77	260	L AnG	
	-40	8	56	4.75	233	L MFG	
	6	-34	54	4.7	220	R MPrG	L MPrG
	44	-58	56	4.63	215	R AnG	
ACE-R (+)	16	-42	34	4.59	112	R PCgG	
	-34	-74	-16	4.61	124	L OFuG	L IOG
	30	-66	-10	4.33	369	R OFuG	R LiG
ACE-R (-)	-30	-22	62	4.29	308	L PrG	L PoG
	-10	-56	-64	4.31	351	L Cer	

Cau, caudate; Cer, cerebellum; FuG, fusiform gyrus; LiG, lingual gyrus; OCP, occipital pole; Plns, posterior insula; Alns, anterior insula; PO, posterior operculum; CO, central operculum; AnG, angular gyrus; MFG, middle frontal gyrus; MPrG, medial precentral gyrus; PCgG, posterior cingulate gyrus; OFuG, occipital fusiform gyrus; IOG, inferior occipital gyrus; PrG, precentral gyrus; PoG, postcentral gyrus; ACE-R, Addenbrooke's Cognitive Examination-Revised; L, left; R, right.

would be more appropriate. As demonstrated in **Figure 2**, regions with significant ICC values were generally consistent with previously identified hubs (Buckner et al., 2009; Sepulcre et al., 2010), thus validating the efficacy of this metric to characterize hub regions and with the mentioned additional advantages.

A related work by Hampson et al. (2012) had investigated age-related changes in the intrinsic connectivity patterns in young and middle aged adults using voxel-level degree measure. They found increases in network degree with age in the paralimbic

cortical and subcortical areas as well as decreases in cortical areas including that in the visual and default mode networks. Consistent with their findings, we found similar increases in whole-brain ICC values with age in the caudate, thalamus, cerebellum, hippocampus, and temporal pole. Moreover, we also found similar decreases in ICC values in the lateral parietal (whole-brain and long-range connections), posterior cingulate (long-range connections) and medial prefrontal (short-range connections). Although there were also differences, these could

be driven by differences in the used metric, the range of age of the study participants, and the number of participants, among other factors.

Characterizing changes in hub regions during normal aging is important since these regions are pivotal in the flow of information within and between networks (Sporns et al., 2007) and are generally implicated in the anatomy of many neurological disorders (Crossley et al., 2014). For instance, Alzheimer's disease (AD) has been shown to selectively target highly connected hub regions in the medial and lateral prefrontal cortices, insula, and thalamus (Dai et al., 2015). The impairment of hub regions was also shown to be connectivity distance-dependent with most disruptions occurring in the long-range connections. Compared to these findings, our results showed that the extent of hub regions involved in aging is somewhat limited. Moreover, most of the regions involved in aging generally differed from that reported in AD, although there were few similarities (left insula, anterior cingulate gyrus, and inferior parietal lobule). Considering also that previous aging studies have reported widespread age-related connectivity changes affecting large-scale brain networks (Betzel et al., 2014; Bagarinao et al., 2019), our findings seemed to suggest that the aging process may mainly affect peripheral non-hub regions, whereas neurodegenerative disorders may predominantly involve connectivity alterations of critical hub regions (Buckner et al., 2009; Dai et al., 2015).

By differentiating the contribution of the different connections in terms of (Euclidean) distance, we were also able to identify differences in hub profiles using distance-dependent ICC values (Figure 2). Similar to a previous study that used network degree to categorize hubs (Sepulcre et al., 2010), we also found that some hub regions were predominantly characterized by their short-range connections (e.g., primary processing systems), whereas others with their long-range connections (e.g., posterior cingulate gyrus and inferior/middle temporal gyrus). In addition, a number of regions such as in the lateral parietal, orbitofrontal gyrus, middle frontal gyrus, and medial superior frontal gyrus showed hub characteristics in both their short-range and long-range connections. Identified hubs with predominant short-range connections are typically located within or near primary sensory or motor areas and may therefore be involved in local information processing. On the other hand, those with predominant long-range connections are regions that have been associated with higher cognitive functions, which require information integration across distributed sources that could be readily achieved using long-range connections. Hub regions that exhibited both short-range and long-range connections are also known association regions, thus the predominant long-range connections are consistent with their known functions. The role of the short-range connections in these hubs, however, remains largely unknown but has been hypothesized as a means to maintain stable *in situ* information while simultaneously being able to associate distributed information with distant connections (Sepulcre et al., 2010).

Given the above, it is not surprising that hubs with predominant long-range connections (e.g., anterior insula, central operculum, and posterior cingulate gyrus) have long-range ICC values that exhibited negative association with

age, whereas those with predominant short-range connections (e.g., fusiform gyrus and anterior cingulate gyrus) have short-range ICC values that were negatively associated with age. Since whole-brain ICC values simply represent the combination of short-range and long-range values, changes in whole-brain ICC values could be a reflection of the changes in connections in either short-range or long-range or both. For example, age-related changes in the anterior insula were observed in both whole-brain and long-range ICC values (Tables 2, 4). From Figure 2, anterior insula is predominantly a long-range hub so that the observed changes in whole-brain ICC values mainly reflected changes in long-range ICC values. In contrast, posterior insula showed changes in both short-range and long-range ICC values and these changes are also being reflected in the whole-brain ICC values (Figures 3a–5a). This could mean that posterior insula's connection to both primary processing systems (sensorimotor/auditory) and salience/BG networks that this region has prominent connections (Figure 3b), could be both affected with age.

Additional seed-based connectivity analyses on regions with ICC values showing significant negative association with age showed that most of the identified regions have connectivity maps that strongly overlapped with not just one but multiple large-scale RSNs. The values of the estimated overlap ratio, computed using whole-brain connections, confirmed that the identified regions are mainly connector hubs, considered important in facilitating information transfer among different brain networks. For instance, the connectivity map of the right medial precentral gyrus overlapped with auditory, sensorimotor, ventral default mode, precuneus, as well as salience networks. Regions in the posterior/anterior insula and posterior/central operculum also overlapped with primary processing networks (sensorimotor, auditory, and primary visual) as well as salience network. These regions are referred to as “control-processing” connector hubs since they linked sensory and motor systems to control networks. Among other functions, control-processing hubs may enable goal-directed control of motor function (Gordon et al., 2018). In contrast, regions in the middle frontal gyrus, angular gyrus, and posterior cingulate gyrus with primarily long-range ICC values that showed significant negative association with age have connectivity maps that strongly overlap with the control (salience, executive, and visuospatial) and default mode networks. These regions are classified as “control-default” connector hubs, which may be responsible for regulating internally generated processes associated with the default mode network such as memories, emotional responses, or planning (Gordon et al., 2018). Age-related alterations of the overall connectivity of these regions could impact its efficiency and thereby affect its functions. Moreover, the effect of aging appeared to vary for different types of connector hubs. Specifically, control-processing connector hubs tend to be affected in both its short-range and long-range (and thus whole-brain) ICC values, whereas control-default connector hubs have primarily long-range ICC values that were negatively associated with age.

In terms of the hubs' association with general cognitive performance, we have identified regions in the visual

and sensorimotor networks with whole-brain and distance-dependent ICC values that showed positive relationship with ACE-R total score. Intriguingly, none of the identified regions overlapped with those having ICC values that negatively associated with age except for a region in the left lingual gyrus, which showed positive relationship with ACE-R total score and negative relationship with age. This finding is consistent with our previous results, which indicated that the integrity of the visual and sensorimotor networks is associated with the participants' general cognitive performance during healthy aging (Bagarinao et al., 2019). In a prospective study of older women, Ward et al. (2018) have also demonstrated that participants with reduced visual function were associated with greater risk of dementia. Physical exercise has also been shown to help improved cognitive function through increased involvement of motor-related networks (Ji et al., 2018). Thus, our finding relating the overall connectivity strength, as quantified by the ICC values, of the primary processing systems to general cognitive performance is consistent with existing literature and provides additional evidence of the importance of the integrity of the primary processing systems during healthy aging for the maintenance of general cognition.

## CONCLUSION

Healthy aging is associated with whole-brain intrinsic functional connectivity changes even in the absence of neurodegenerative diseases. Using ICC, we have identified a limited number of regions with overall connectivity strength that showed significant negative relationship with age. More importantly, these regions have functional connectivity profiles that significantly overlapped with not just one but multiple large-scale RSNs indicating that these regions are connector hubs. Connector hubs associated with primary processing (sensorimotor, visual, and auditory) and control networks tended to have whole-brain ICC values that exhibited significant negative relationship with age, whereas control-default connector hubs have predominantly long-range ICC values that exhibited significant negative relationship with age. These findings suggest that even healthy aging could negatively impact, albeit in a limited way, the overall connectivity strength of regions critical in facilitating information transfer among different networks.

## DATA AVAILABILITY STATEMENT

The datasets presented in this article are not readily available because of privacy and ethical restrictions. Requests to access the datasets should be directed to GS, sobueg@med.nagoya-u.ac.jp.

## REFERENCES

- Achard, S., and Bullmore, E. (2007). Efficiency and cost of economical brain functional networks. *PLoS Comput. Biol.* 3:e17. doi: 10.1371/journal.pcbi.0030017
- Achard, S., Salvador, R., Whitcher, B., Suckling, J., and Bullmore, E. (2006). A resilient, low-frequency, small-world human brain functional network with highly connected association cortical hubs. *J. Neurosci.* 26, 63–72. doi: 10.1523/JNEUROSCI.3874-05.2006
- Alexander-Bloch, A. F., Vértes, P. E., Stidd, R., Lalonde, F., Clasen, L., Rapoport, J., et al. (2013). The anatomical distance of functional connections predicts brain network topology in health and schizophrenia. *Cereb. Cortex* 23, 127–138. doi: 10.1093/cercor/bhr388

## ETHICS STATEMENT

The studies involving human participants were reviewed and approved by the Ethics Committee of Nagoya University Graduate School of Medicine. The patients/participants provided their written informed consent to participate in this study.

## AUTHOR CONTRIBUTIONS

HW, SM, TT, HT, MKa, TW, MKu, MH, HI, SN, NO, and GS contributed to conception and design of the study. SM, DM, KH, KK, NY, RO, KI, MM, TY, AO, SK, MH, and HI were involved in data acquisition, data organization, and data curation. EB, HW, KK, TT, and HT contributed to the methodology, analysis, and interpretation of the data. EB, HW, SM, and GS wrote the draft of the manuscript. All authors reviewed and approved the final version of the manuscript.

## FUNDING

This work was supported by Grants-in-Aid from the Research Committee of Central Nervous System Degenerative Diseases by the Ministry of Health, Labour, and Welfare and from the Integrated Research on Neuropsychiatric Disorders project carried out under the Strategic Research for Brain Sciences by the Ministry of Education, Culture, Sports, Science, and Technology of Japan. This work was also supported by a Grant-in-Aid for Scientific Research from the Ministry of Education, Culture, Sports, Science, and Technology (MEXT) of Japan (grant number: 80569781), and a Grant-in-Aid for Scientific Research on Innovative Areas (Brain Protein Aging and Dementia Control) (grant number: 26117002) from MEXT. The funders had no role in study design, data collection, analysis, and interpretation, preparation of the manuscript, or decision to publish.

## SUPPLEMENTARY MATERIAL

The Supplementary Material for this article can be found online at: <https://www.frontiersin.org/articles/10.3389/fnagi.2020.592469/full#supplementary-material>

- Andrews-Hanna, J. R., Snyder, A. Z., Vincent, J. L., Lustig, C., Head, D., Raichle, M. E., et al. (2007). Disruption of large-scale brain systems in advanced aging. *Neuron* 56, 924–935. doi: 10.1016/j.neuron.2007.10.038
- Ashburner, J., and Friston, K. J. (2005). Unified segmentation. *Neuroimage* 26, 839–851. doi: 10.1016/j.neuroimage.2005.02.018
- Bagarinao, E., Watanabe, H., Maesawa, S., Mori, D., Hara, K., Kawabata, K., et al. (2018). An unbiased data-driven age-related structural brain parcellation for the identification of intrinsic brain volume changes over the adult lifespan. *Neuroimage* 169, 134–144. doi: 10.1016/j.neuroimage.2017.12.014
- Bagarinao, E., Watanabe, H., Maesawa, S., Mori, D., Hara, K., Kawabata, K., et al. (2019). Reorganization of brain networks and its association with general cognitive performance over the adult lifespan. *Sci. Rep.* 9:11352. doi: 10.1038/s41598-019-47922-x
- Bagarinao, E., Watanabe, H., Maesawa, S., Mori, D., Hara, K., Kawabata, K., et al. (2020). Identifying the brain's connector hubs at the voxel level using functional connectivity overlap ratio. *Neuroimage* 222:117241. doi: 10.1016/j.neuroimage.2020.117241
- Beckmann, C. F., DeLuca, M., Devlin, J. T., and Smith, S. M. (2005). Investigations into resting-state connectivity using independent component analysis. *Philos. Trans. R. Soc. B Biol. Sci.* 360, 1001–1013. doi: 10.1098/rstb.2005.1634
- Betzler, R. F., Byrge, L., He, Y., Goñi, J., Zuo, X. N., and Sporns, O. (2014). Changes in structural and functional connectivity among resting-state networks across the human lifespan. *Neuroimage* 102, 345–357. doi: 10.1016/j.neuroimage.2014.07.067
- Biswal, B., Yetkin, F. Z., Haughton, V. M., and Hyde, J. S. (1995). Functional connectivity in the motor cortex of resting human brain using echo-planar MRI. *Magn. Reson. Med.* 34, 537–541. doi: 10.1002/mrm.1910340409
- Buckner, R. L., Sepulcre, J., Talukdar, T., Krienen, F. M., Liu, H., Hedden, T., et al. (2009). Cortical hubs revealed by intrinsic functional connectivity: mapping, assessment of stability, and relation to Alzheimer's disease. *J. Neurosci.* 29, 1860–1873. doi: 10.1523/JNEUROSCI.5062-08.2009
- Bullmore, E., and Sporns, O. (2012). The economy of brain network organization. *Nat. Rev. Neurosci.* 13, 336–349. doi: 10.1038/nrn3214
- Chan, M. Y., Park, D. C., Savalia, N. K., Petersen, S. E., and Wig, G. S. (2014). Decreased segregation of brain systems across the healthy adult lifespan. *Proc. Natl. Acad. Sci. U.S.A.* 111, E4997–E5006. doi: 10.1073/pnas.1415122111
- Crossley, N. A., Mechelli, A., Scott, J., Carletti, F., Fox, P. T., McGuire, P., et al. (2014). The hubs of the human connectome are generally implicated in the anatomy of brain disorders. *Brain* 137, 2382–2395. doi: 10.1093/brain/awu132
- Dai, Z., Yan, C., Li, K., Wang, Z., Wang, J., Cao, M., et al. (2015). Identifying and mapping connectivity patterns of brain network hubs in Alzheimer's disease. *Cereb. Cortex* 25, 3723–3742. doi: 10.1093/cercor/bhu246
- Fransson, P., Skold, B., Horsch, S., Nordell, A., Blennow, M., Lagercrantz, H., et al. (2007). Resting-state networks in the infant brain. *Proc. Natl. Acad. Sci. U.S.A.* 104, 15531–15536. doi: 10.1073/pnas.0704380104
- Geerligs, L., Renken, R. J., Saliasi, E., Maurits, N. M., and Lorist, M. M. (2015). A Brain-wide study of age-related changes in functional connectivity. *Cereb. Cortex* 25, 1987–1999. doi: 10.1093/cercor/bhu012
- Gordon, E. M., Lynch, C. J., Gratton, C., Laumann, T. O., Gilmore, A. W., Greene, D. J., et al. (2018). Three distinct sets of connector hubs integrate human brain function. *Cell Rep.* 24, 1687–1695.e4. doi: 10.1016/j.celrep.2018.07.050
- Greicius, M. (2008). Resting-state functional connectivity in neuropsychiatric disorders. *Curr. Opin. Neurol.* 21, 424–430. doi: 10.1097/wco.0b013e328306f2c5
- Greicius, M. D., Krasnow, B., Reiss, A. L., and Menon, V. (2003). Functional connectivity in the resting brain: a network analysis of the default mode hypothesis. *Proc. Natl. Acad. Sci. U.S.A.* 100, 253–258. doi: 10.1073/pnas.0135058100
- Greicius, M. D., Srivastava, G., Reiss, A. L., and Menon, V. (2004). Default-mode network activity distinguishes Alzheimer's disease from healthy aging: evidence from functional MRI. *Proc. Natl. Acad. Sci. U.S.A.* 101, 4637–4642. doi: 10.1073/pnas.0308627101
- Hacker, C. D., Perlmutter, J. S., Criswell, S. R., Ances, B. M., and Snyder, A. Z. (2012). Resting state functional connectivity of the striatum in Parkinson's disease. *Brain* 135, 3699–3711. doi: 10.1093/brain/aww281
- Hampson, M., Tokoglu, F., Shen, X., Scheinost, D., Papademetris, X., and Constable, R. T. (2012). Intrinsic Brain connectivity related to age in young and middle aged adults. *PLoS One* 7:e44067. doi: 10.1371/journal.pone.0044067
- He, Y., Chen, Z. J., and Evans, A. C. (2007). Small-world anatomical networks in the human brain revealed by cortical thickness from MRI. *Cereb. Cortex* 17, 2407–2419. doi: 10.1093/cercor/bhl149
- Ji, L., Pearlson, G. D., Zhang, X., Steffens, D. C., Ji, X., Guo, H., et al. (2018). Physical exercise increases involvement of motor networks as a compensatory mechanism during a cognitively challenging task. *Int. J. Geriatr. Psychiatry* 33, 1153–1159. doi: 10.1002/gps.4909
- Jones, D. T., MacHulda, M. M., Vemuri, P., McDade, E. M., Zeng, G., Senjem, M. L., et al. (2011). Age-related changes in the default mode network are more advanced in Alzheimer disease. *Neurology* 77, 1524–1531. doi: 10.1212/WNL.0b013e318233b33d
- Kawabata, K., Watanabe, H., Hara, K., Bagarinao, E., Yoneyama, N., Ogura, A., et al. (2018). Distinct manifestation of cognitive deficits associate with different resting-state network disruptions in non-demented patients with Parkinson's disease. *J. Neurol.* 265, 688–700. doi: 10.1007/s00415-018-8755-5
- Liang, X., Zou, Q., He, Y., and Yang, Y. (2013). Coupling of functional connectivity and regional cerebral blood flow reveals a physiological basis for network hubs of the human brain. *Proc. Natl. Acad. Sci. U.S.A.* 110, 1929–1934. doi: 10.1073/pnas.1214900110
- Martuzzi, R., Ramani, R., Qiu, M., Shen, X., Papademetris, X., and Constable, R. T. (2011). A whole-brain voxel based measure of intrinsic connectivity contrast reveals local changes in tissue connectivity with anesthetic without a priori assumptions on thresholds or regions of interest. *Neuroimage* 58, 1044–1050. doi: 10.1016/j.neuroimage.2011.06.075
- Menon, V. (2011). Large-scale brain networks and psychopathology: a unifying triple network model. *Trends Cogn. Sci.* 15, 483–506. doi: 10.1016/j.tics.2011.08.003
- Mugler, J. P., and Brookeman, J. R. (1990). Three-dimensional magnetization-prepared rapid gradient-echo imaging (3D MP RAGE). *Magn. Reson. Med.* 15, 152–157. doi: 10.1002/mrm.1910150117
- Ogura, A., Watanabe, H., Kawabata, K., Ohdake, R., Tanaka, Y., Masuda, M., et al. (2019). Semantic deficits in ALS related to right lingual/fusiform gyrus network involvement. *Ebiomedicine* 47, 506–517. doi: 10.1016/j.ebiom.2019.08.022
- Power, J. D., Barnes, K. A., Snyder, A. Z., Schlaggar, B. L., and Petersen, S. E. (2012). Spurious but systematic correlations in functional connectivity MRI networks arise from subject motion. *Neuroimage* 59, 2142–2154. doi: 10.1016/j.neuroimage.2011.10.018
- Sala-Llonch, R., Bartrés-Faz, D., and Junqué, C. (2015). Reorganization of brain networks in aging: a review of functional connectivity studies. *Front. Psychol.* 6:663. doi: 10.3389/fpsyg.2015.00663
- Seeley, W. W., Menon, V., Schatzberg, A. F., Keller, J., Glover, G. H., Kenna, H., et al. (2007). Dissociable intrinsic connectivity networks for salience processing and executive control. *J. Neurosci.* 27, 2349–2356. doi: 10.1523/JNEUROSCI.5587-06.2007
- Sepulcre, J., Liu, H., Talukdar, T., Martincorena, I., Yeo, B. T. T., and Buckner, R. L. (2010). The organization of local and distant functional connectivity in the human brain. *PLoS Comput. Biol.* 6:e1000808. doi: 10.1371/journal.pcbi.1000808
- Shirer, W. R., Ryali, S., Rykhlevskaia, E., Menon, V., and Greicius, M. D. (2012). Decoding subject-driven cognitive states with whole-brain connectivity patterns. *Cereb. Cortex* 22, 158–165. doi: 10.1093/cercor/bhr099
- Smith, S. M., Miller, K. L., Salimi-Khorshidi, G., Webster, M., Beckmann, C. F., Nichols, T. E., et al. (2011). Network modelling methods for FMRI. *Neuroimage* 54, 875–891. doi: 10.1016/j.neuroimage.2010.08.063
- Smyser, C. D., Inder, T. E., Shimony, J. S., Hill, J. E., Degnan, A. J., Snyder, A. Z., et al. (2010). Longitudinal analysis of neural network development in preterm infants. *Cereb. Cortex* 20, 2852–2862. doi: 10.1093/cercor/bhq035
- Song, J., Birn, R. M., Boly, M., Meier, T. B., Nair, V. A., Meyerand, M. E., et al. (2014). Age-related reorganizational changes in modularity and functional connectivity of human brain networks. *Brain Connect.* 4, 662–676. doi: 10.1089/brain.2014.0286
- Sporns, O., Honey, C. J., and Kötter, R. (2007). Identification and classification of hubs in brain networks. *PLoS One* 2:e1049. doi: 10.1371/journal.pone.0001049
- Tomasí, D., and Volkow, N. D. (2012). Aging and functional brain networks. *Mol. Psychiatry* 17, 549–558. doi: 10.1038/mp.2011.81

- van den Heuvel, M. P., and Sporns, O. (2013). Network hubs in the human brain. *Trends Cogn. Sci.* 17, 683–696. doi: 10.1016/j.tics.2013.09.012
- van den Heuvel, M. P., Sporns, O., Collin, G., Scheewe, T., Mandl, R. C. W., Cahn, W., et al. (2013). Abnormal rich club organization and functional brain dynamics in schizophrenia. *JAMA Psychiatry* 70, 783–792. doi: 10.1001/jamapsychiatry.2013.1328
- Ward, M. E., Gelfand, J. M., Lui, L.-Y., Ou, Y., Green, A. J., Stone, K., et al. (2018). Reduced contrast sensitivity among older women is associated with increased risk of cognitive impairment. *Ann. Neurol.* 83, 730–738. doi: 10.1002/ana.25196
- Xia, M., Wang, J., and He, Y. (2013). BrainNet viewer: a network visualization tool for human brain connectomics. *PLoS One* 8:e68910. doi: 10.1371/journal.pone.0068910
- Yao, N., Shek-Kwan Chang, R., Cheung, C., Pang, S., Lau, K. K., Suckling, J., et al. (2014). The default mode network is disrupted in parkinson's disease with visual hallucinations. *Hum. Brain Mapp.* 35, 5658–5666. doi: 10.1002/hbm.22577
- Yokoi, T., Watanabe, H., Yamaguchi, H., Bagarinao, E., Masuda, M., Imai, K., et al. (2018). Involvement of the Precuneus/posterior cingulate cortex is significant for the development of Alzheimer's disease: a PET (THK5351, PiB) and resting fMRI study. *Front. Aging Neurosci.* 10:304. doi: 10.3389/fnagi.2018.00304
- Yoneyama, N., Watanabe, H., Kawabata, K., Bagarinao, E., Hara, K., Tsuboi, T., et al. (2018). Severe hyposmia and aberrant functional connectivity in cognitively normal Parkinson's disease. *PLoS One* 13:e0190072. doi: 10.1371/journal.pone.0190072

**Conflict of Interest:** The authors declare that the research was conducted in the absence of any commercial or financial relationships that could be construed as a potential conflict of interest.

Copyright © 2020 Bagarinao, Watanabe, Maesawa, Mori, Hara, Kawabata, Yoneyama, Ohdake, Imai, Masuda, Yokoi, Ogura, Taoka, Koyama, Tanabe, Katsuno, Wakabayashi, Kuzuya, Hoshiyama, Isoda, Naganawa, Ozaki and Sobue. This is an open-access article distributed under the terms of the Creative Commons Attribution License (CC BY). The use, distribution or reproduction in other forums is permitted, provided the original author(s) and the copyright owner(s) are credited and that the original publication in this journal is cited, in accordance with accepted academic practice. No use, distribution or reproduction is permitted which does not comply with these terms.